HHS Public Access

Author manuscript

*Nat Struct Mol Biol*. Author manuscript; available in PMC 2009 January 01.

Published in final edited form as:

*Nat Struct Mol Biol*. 2008 July ; 15(7): 700–706. doi:10.1038/nsmb.1433.

# Supramolecular SNARE assembly precedes hemifusion in SNARE-mediated membrane fusion

**Xiaobing Lu**[1,2], **Yinghui Zhang**[1,2], and **Yeon-Kyun Shin**[1]

[1] Department of Biochemistry, Biophysics and Molecular Biology, Molecular Biology Building, Iowa State University, Ames, Iowa 50011, USA

## Abstract

Formation of the soluble N-ethylmaleimide-sensitive factor attachment protein receptor (SNARE) complex facilitates intracellular membrane fusion. A single SNARE complex is thought to be insufficient; multiple copies of SNARE complexes must work cooperatively. However, the mechanism by which such a higher-order SNARE protein structure is assembled is unknown. EPR and fluorescence analyses show that at least three copies of target-membrane SNARE proteins self-assemble through the interaction between the transmembrane domains (TMDs), and this multimeric structure serves as scaffolding for trans-SNARE assembly. SNARE core formation in solution induces oligomerization of the TMDs of vesicle-associated SNAREs in the apposing membrane, transiently forming a supramolecular protein structure spanning two membranes. This higher-order protein intermediate evolves, by involving lipid molecules, to the hemifusion state. Hemifusion is subsequently followed by distal leaflet mixing and formation of the cis-SNARE complex.

Snare-mediated membrane fusion underlies intracellular protein trafficking and intercellular communication such as neurotransmission1–4. Molecular recognition between vesicle-associated SNARE (v-SNARE) and target-membrane SNARE (t-SNARE) leads to formation of a coiled coil that bridges two membranes5–11. Successful membrane fusion, however, requires cooperative action of multiple copies of SNARE complexes12–16. One obvious reason for such cooperative action is to overcome the repulsion between two apposing membranes17. The TMDs are thought to play a role in driving oligomerization of SNARE complexes18–22. Although the past work revealed information about the likely stoichiometric number of the SNARE oligomers, the process whereby SNARE oligomerization occurs remains to be understood.



Correspondence should be addressed to Y.-K.S. (colishin@iastate.edu).

[2]These authors contributed equally to this work.

Published online at http://www.nature.com/nsmb/

Reprints and permissions information is available online at http://npg.nature.com/reprintsandpermissions/

AUTHOR CONTRIBUTIONS

X.L. performed the fluorescence assay; Y.Z. performed the EPR analysis. Y.-K.S. designed the experiment and wrote the paper.

Oligomerization of SNARE complexes at the onset of membrane fusion may have functional implications for some exocytotic events, such as neurotransmitter release. A gap junction–like arrangement of multiple SNARE complexes may allow a narrow protein pore to traverse two membranes, which is possibly the source of a small 'foot current' observed in the electrophysiological measurements21,23,24.

Recently, progress has been made in understanding the transitions that lipids experience during membrane fusion. There is compelling evidence that SNARE-mediated fusion transits through the hemifusion state in which proximal leaflets are merged while the distal leaflets remain unchanged25–33. The hemifusion state progresses to full fusion possibly after a few flickers between the hemifusion and the small-pore states25. Recently, it has been shown that hemifusion may have important biological implications. For example, in sea urchin, the cortical granules are hemifused before fusion with the egg plasma membrane31. In neurons, most synaptic vesicles are in the hemifused state on the presynaptic plasma membrane34.

It is often argued, for certain energetic reasons, that a gap junction–like protein intermediate is incompatible with a hemifusion intermediate in the fusion pathway17. Therefore, two seemingly mutually exclusive mechanistic models, one based on the hemifusion intermediate25,28,29,35,36 and the other built around the protein pore37–39, have been developed for SNARE-mediated membrane fusion. In this work, we show that both the two-membrane-spanning protein intermediate and the hemifused state do exist sequentially along the fusion pathway. We also investigate the mechanism by which the supramolecular SNARE structure is formed for yeast SNAREs.

## RESULTS

### TMDs of t-SNARE self-assemble to form an oligomer

We studied SNAREs that play a role in trafficking in yeast. Yeast SNAREs share functional and structural similarities with neuronal SNAREs that are involved in synaptic membrane fusion. Sso1p and Sec9 are t-SNAREs analogous to neuronal Syntaxin 1A and SNAP-25, respectively. Sso1p has a transmembrane domain that anchors the t-SNARE to the membrane (Fig. 1a). Snc2p is the yeast counterpart of the neuronal v-SNARE synaptobrevin (VAMP). For simplicity, we used shorter versions of the t-SNAREs Sso1pHT and Sec9c. Sso1pHT lacks the N-terminal regulatory Habc domain and Sec9c contains only the region homologous to SNAP-25 (see Methods section).

It has previously been shown that there is a weak interaction among Sso1pHT TMDs in the membrane that results in an equilibrium between the monomeric form and the multimeric form40. Here, we used site-directed spin labeling (SDSL) and EPR to analyze this equilibrium quantitatively. In SDSL, native amino acid residues are replaced one by one with cysteine to which a nitroxide side chain is attached. The EPR line shape is sensitive to the motional rates of the nitroxide. For monomeric Sso1pHT, no tertiary interaction would be expected for residues in the TMD, which should result in relatively narrow EPR spectra reflecting fast motion of the nitroxide side chain. For homo-oligomeric Sso1pHT, by

contrast, we expect tertiary contacts for several TMD positions, which would instead result in broad EPR spectra reflecting retarded motion of the nitroxide side chain.

In equilibrium, the monomers coexist with the multimers, which, for those positions with tertiary contacts, gives rise to composite EPR spectra composed of a sharp component representing the monomer and a broad component representing the multimer (Fig. 1b). As a first approximation, we assume that equilibrium is between the monomeric species and a single multimeric form with the stoichiometric number *n*:

$$nM \overset{K}{\longleftrightarrow} M_n \quad (1)$$

where *K* represents the equilibrium constant. Based on this simple two-state model, the fraction of the homomultimer *f* and that of the monomer (1 – *f*) are readily obtained using a standard EPR spectral subtraction analysis (Fig. 1b).

We performed EPR spectral analysis for four different TMD positions (269, 272, 273 and 284), which showed clear tertiary interactions in the EPR spectra40. The *f* values were calculated at four different surface protein densities (lipid:protein ratio = 400:1, 200:1, 100:1, 50:1), for each spin-labeled mutant reconstituted into 1-palmitoyl-2-dioleoyl-*sn*-glycero-3-phosphatidylcholine (POPC) vesicles containing 15 molar percent negatively charged 1,2-dioleoyl-*sn*-glycero-3-phosphatidylserine (DOPS). The variation of *f* as a function of *C* was collectively fitted to equation (1) (see Methods) to determine the best-fitting values of *n* and *K*. The best-fitting *n* value was four (Fig. 1c). However, other *n* values, except *n* = 2, also fit the data reasonably well, although the corresponding statistical tests were somewhat poorer (Supplementary Table 1 online). Therefore, we conclude that at least three Sso1pHT molecules self-associate to form the oligomer. The composite EPR spectra were not altered at all by the addition of Sec9c at all lipid:protein ratios for each mutant, indicating that the equilibrium properties observed for Sso1pHT alone are virtually the same for t-SNARE.

## SNARE assembly versus oligomerization of the v-SNARE TMDs

Our EPR results showed that at least three copies of the Sso1pHT TMD clustered together to form a homo-oligomeric structure in the membrane. In contrast, it has previously been shown that the TMDs of v-SNARE Snc2p exist as monomers28. Therefore, we wondered whether multimeric Sso1pHT provides scaffolding for formation of the initial fusion complex at the fusion active zone. Thus, we used site-specific fluorescence labeling to investigate the dynamic changes occurring during SNARE assembly and membrane fusion. As with the EPR, we used cysteine-free versions of Sso1pHT and Snc2p to generate two N-terminal mutants, Sso1pHT E185C (Nt) and Snc2p P13C (Nv), and two C-terminal mutants, Sso1pHT R290C (Ct) and Snc2p S115C (Cv). The Sso1pHT mutants were derivatized with the fluorescence donor Cy3 maleimide, while the Snc2p mutants were reacted with the acceptor Cy5 maleimide. The labeled proteins were reconstituted into the POPC vesicle containing 35 molar percent negatively charged DOPS.

The fusion reaction was conveniently initiated by adding Sec9c to a mixture of t-SNARE vesicles and v-SNARE vesicles. We first monitored SNARE complex formation using Nt-

Cy3 and Nv-Cy5. Upon addition of Sec9c, we observed a rapid increase of fluorescence for the acceptor Cy5 and a rapid decrease for the donor Cy3, indicating that fluorescence resonance energy transfer (FRET) occurred owing to formation of the SNARE core (Fig. 2a). As controls, when the t-SNARE vesicles with Nt-Cy3 were mixed with the unlabeled v-SNARE vesicles or vice versa, we did not observe any substantial spectral changes in time (Fig. 2b), suggesting that the observed fluorescence changes were mainly due to the energy transfer from the fluorescence donor to the acceptor. Likewise, when the t-SNARE vesicles with Ct-Cy3 were reacted with the unlabeled v-SNARE vesicles by adding Sec9c, we detected no fluorescence change, suggesting that the TMDs of Sso1pHT remained unchanged during SNARE core formation. In contrast, when the v-SNARE vesicles carrying Cv-Cy5 were reacted with unlabeled t-SNARE vesicles, the fluorescence intensity decreased rapidly, suggesting the possibility of self-quenching due to the self-association of v-SNARE TMDs in the membrane. Of special note, the kinetics of this particular fluorescence change matched that of SNARE assembly detected at the N-terminal tip of the SNARE core, showing that the change reported by Cv-Cy5 at the C-terminal end occurs concurrently with SNARE complex formation.

To make sure that the observed fluorescence change was due to the change in the inter-TMD interactions, rather than to environmental changes surrounding individual TMDs, we diluted Cv-Cy5 with a threefold excess of wild-type Snc2p before reconstitution into vesicles. We observed no fluorescence change for this diluted sample (Supplementary Fig. 1 online), supporting the ideas that the fluorescence change here is most likely due to self-quenching and that the TMDs of Snc2p self-associate during SNARE assembly. Therefore, as self-quenching was not observed on the fluorescent label attached to either the N or C termini of t-SNARE Sso1pHT, but it was observed on the fluorescent label attached to the C terminus of v-SNARE Snc2p, the results strongly support the idea that the Sso1pHT oligomer recruits Snc2p to the fusion active zone to form a supramolecular SNARE complex that traverses two closely apposed membranes.

## Supramolecular SNARE assembly is followed by hemifusion

How do the changes in SNARE structure correlate with the changes in membrane structure? There is evidence that SNARE-mediated fusion transits through the hemifusion intermediate25–33. We asked whether hemifusion was concurrent with or sequential to formation of the initial supramolecular complex. Lipid mixing was measured by a well established method using fluorescent lipids (see Methods). Membrane fusion causes the dilution of the fluorescent probes, which can be measured as the recovery of the donor fluorescence signal. To detect hemifusion, it is necessary to separate outer-leaflet mixing from inner-leaflet mixing. Such separation can be achieved by independently measuring total lipid mixing, which is the sum of inner and outer leaflet mixing, and inner leaflet mixing. We measured inner leaflet mixing with the modification of a previously published method using dithionite reduction of NBD on the outer leaflet to nonfluorescent ABD (7-amino-2,1,3-benzoxadia-zol-4-yl)41. Outer leaflet mixing occurred faster than inner leaflet mixing (Fig. 3), confirming the existence of the hemifusion intermediate. Further, when the kinetics of outer leaflet mixing was compared with that of clustering of v-SNARE TMDs, the former was seen to occur slower than the latter (Fig. 4). The quantitative analysis of the

data based on second-order kinetics (Fig. 4a) showed that the second-order rate constant $k_2$ of supramolecular SNARE assembly was about four times faster than that of hemifusion (Fig. 4b). Thus, the results show that hemifusion follows formation of the initial fusion complex sequentially.

### *cis*-SNARE complex formation versus inner leaflet mixing

In the membrane fusion pathway, hemifusion is followed by opening of the fusion pore. Pore opening accompanies inner leaflet mixing. Further, the v- and t-SNARE TMDs merge into the same bilayer to form the *cis*-SNARE complex. We expected that formation of the *cis*-SNARE complex would occur concurrently with inner leaflet mixing. To verify this, we used C-terminally labeled t- and v-SNAREs in our FRET fusion assay. We first reconstituted the mixture of Cv-Cy5 and wild-type Snc2p in the ratio of 1:3 into one population of vesicles. We then reacted these vesicles with another population of vesicles containing Ct-Cy3 and wild-type Sso1pHT in the ratio of 1:3. In this experiment, we diluted the labeled proteins with the corresponding wild-type proteins to avoid potential complications arising from self-quenching. When Sec9c was added to the reaction, an increase of the fluorescence intensity in the acceptor channel (Cy5) and a decrease of the fluorescence intensity in the donor channel (Cy3) were observed (Fig. 4c). The results show that the distance between Cy5 and Cy3 was decreased, most likely due to the colocalization of v- and t-SNARE TMDs in the newly merged, single bilayer. The timescale of the fluorescence change was consistent with that of inner leaflet mixing (Fig. 4). Therefore, we conclude that formation of the *cis*-SNARE complex occurs concurrently with inner leaflet mixing but slower than hemifusion. The data analysis (Fig. 4a) showed that the $k_2$ value of *cis*-SNARE complex formation is about three times slower than that of hemifusion (Fig. 4b). The data are, however, insufficient to tell whether there was association between the v- and t-SNARE TMDs because FRET can be observed over the several-nanometer range in the absence of physical contacts.

## DISCUSSION

SNARE complex formation may drive membrane fusion. A recent force measurement, however, showed that the energy from a single SNARE complex might not be sufficient to overcome the full fusion energy barrier42. Therefore, multimerization of SNAREs seems to be essential for successful fusion. The existence of higher-order SNARE complexes has been consistently confirmed in squid synaptosomes and brain by extraction43 as well as in artificial membrane by atomic force microscopy44.

Quantitatively, a kinetic analysis of exocytosis in cracked PC12 cells shows that at least three SNARE complexes work together for membrane fusion12. Based on the EPR analysis of the equilibrium between the Sso1pHT TMD monomers and the oligomers, we estimated the likely stoichiometry of the TMD oligomer for yeast SNAREs to be three or higher, which is fully consistent with previous results for neuronal SNAREs12.

We used fluorescence self-quenching between identical probes to assess the clustering of the v-SNARE TMDs, which is driven by SNARE core formation. Self-quenching is photophysically different from homo-FRET between two identical dyes. Whereas homo-

FRET can measure distances up to 3–6 nm by analyzing fluorescence polarization45, self-quenching requires close physical proximity between dyes and is visible only when the dyes are within ~1 nm (refs. 46,47). Therefore, the self-quenching observed at the C terminus of Snc2p is a strong indicator for self-association of the v-SNARE TMDs in the membrane.

The combined EPR and fluorescence analysis of SNARE assembly showed that the very early fusion intermediate might be a protein-only supramolecular SNARE complex that spanned two membranes (Fig. 5a,b). Such a protein intermediate would be assembled through a dynamic process in which the preformed t-SNARE homo-oligomer recruits v-SNAREs through SNARE complex formation (Fig. 5a,b). Formation of a gap junction–like protein pore for neuronal SNAREs at the onset of membrane fusion has previously been predicted, with little direct evidence21,37. This hypothetical transient protein pore was envisioned as harboring an early aqueous passage through which small amounts of neurotransmitters could be released from the synaptic vesicle to the synapse. It is unknown, however, whether the initial fusion complex formed by yeast SNAREs harbors such a pore within the supramolecular structure.

Our results clearly demonstrate that hemifusion sequentially follows formation of the transient protein intermediate (Fig. 5c). How does the assembly go from the protein-only supramolecular structure to the lipid-rich hemifusion state? It is possible that a lipid stalk-like state emerges at the center of the protein complex (Fig. 5c), which requires the lateral diffusion of the individual TMDs into the lipid matrix. In this process, the lipid molecules would be fed into the central zone to establish a stalk-like structure in the middle. Favoring this model, the Sso1pHT TMDs are held together by weak interactions40, and therefore such lateral diffusion of the TMDs can occur naturally as part of the equilibrium fluctuation between the monomeric TMD and the oligomeric form. We speculate that this hypothetical stalk corralled by the SNARE TMDs is lower in free energy than a lipid-only stalk. Alternatively, outer leaflet mixing can occur through the hydrophobic surface of the transient protein complex37. Even in this case, the lipid molecules must be fed into the central zone during the lateral expansion of the TMDs. It is hard to imagine, for energetic reasons, that the lipids in the central region form the lipid-lined pore directly without forming an initial stalk-like structure17. At minimum, for SNARE-mediated fusion, the lipid-only stalk model must be revised to incorporate the presence of the TMDs that are concentrated in high numbers in the fusion active zone.

The hemifusion state transitions to the fusion pore, which completes the merging of the two membranes (Fig. 5d). It is reasonable to expect the disruption of the SNARE TMD oligomer at this stage. In our EPR data, several positions in the Sso1pHT TMD, including 269, 273, 276, 281, 282, 286, 287 and 288, showed a reduction of the broad components in the *cis*-SNARE complex compared to those for Sso1pHT alone (Supplementary Fig. 2 online). The decrease of the broad components may reflect the dissociation of the Sso1pHT TMD oligomer. In our fluorescence experiment, however, we did not observe self-dequenching from C-terminally labeled Sso1pHT reflecting such dissociation of the TMD oligomer during fusion. One possible explanation for this is that in the bulk fusion assay, most of the vesicles remain in the docked state. Only about 10% of docked vesicles progress to the hemifused or fully fused states, while 90% of them remain docked without fusion. In the

docked state, we predict that the SNARE complex maintains the oligomeric form. Because only a small fraction of vesicles would show dissociation due to fusion, the change may be too small to be detectable in our bulk fusion assay. The recently developed single fusion assay25 may be used to resolve this issue. In this method, the docking and subsequent fusion steps are clearly resolved in individual fusion events and the expected dissociation of the TMDs can be readily detected.

Using FRET, we found that inner leaflet mixing was concurrent with formation of the *cis*-SNARE complex, indicating that the *trans*-to-*cis* transition of the SNARE TMDs may be closely correlated with fusion pore opening. Our results also suggest that during inner leaflet mixing the fluorescent dyes in the two separate vesicles cross the aqueous pore so that they could be co-located on a newly merged single membrane.

The analysis of the kinetic data (Fig. 4b) showed that the second-order rate constant $k_2$ for inner leaflet mixing was three times slower than that for outer leaflet mixing. This result implies that the activation energy of the former is ~0.7 kcal $mol^{-1}$ higher than that of the latter. SNARE complex formation must provide the energy required to overcome the activation energy barriers for both hemifusion and pore opening. Supposing that SNARE core formation drives primarily hemifusion42, where, then, does the extra energy for pore opening come from after hemifusion? Hypothetically, the energy from the SNARE complex may be released in two steps: initially for hemifusion and later for pore opening. A single-molecule force measurement has shown the possibility of such stepwise release of the energy through two-step assembly of the SNARE core complex, the membrane-distal region first and the membrane-proximal region later42.

## METHODS

### Plasmids and site-directed mutagenesis

DNA sequences encoding Sso1pHT (amino acids 185–290 of Sso1p) and Snc2p (amino acids 1–115) were inserted into the pGEX-KG vector between EcoRI and HindIII sites as N-terminal glutathione S-transferase (GST) fusion proteins. A DNA sequence encoding Sec9c (amino acids 401–651 of Sec9) was inserted into pET-24b(+) between the NdeI and XhoI sites as a C-terminally $His_6$-tagged protein. To leave a unique cysteine residue for the specific nitroxide attachment, the native Cys266 of Sso1pHT was mutated to alanine. We used the Quick Change site-directed mutagenesis kit (Stratagene) to generate all cysteine mutants; DNA sequences were confirmed by the Iowa State University DNA Sequencing Facility.

### Protein expression, purification and labeling

Expression of recombinant GST fusion proteins was conducted in *Escherichia coli* Rosetta (DE3) pLysS (Novagene). Cells were grown at 37 °C in LB medium with glucose (2 g $liter^{-1}$), ampicillin (100 μg $ml^{-1}$) and chloramphenicol (25 μg $ml^{-1}$) until the absorbance at 600 nm reached 0.6–0.8. IPTG (1 mM final concentration) was then added to induce protein expression. Cells were grown for another 4 h at 16 °C. Cell pellets were then collected by centrifugation at 5,500*g* for 10 min.

Purification of GST fusion proteins was achieved with affinity chromatography using glutathione-agarose beads (Sigma). The frozen cell pellets were resuspended in PBS buffer, pH 7.4, containing 0.2% (v/v) Triton X-100, 2 mM 4-(2-aminoethyl)-benzenesulfonyl fluoride (AEBSF) and 5 mM DTT. Cells were broken by sonication in an ice bath and then centrifuged at 14,500*g* for 20 min at 4 °C. The supernatant was mixed with the glutathione-agarose beads in the same buffer and nutated at 4 °C for 120 min. The protein was cleaved from the resin by thrombin (Sigma) at room temperature for 40 min. The protein was stored at −80 °C with 10% (v/v) glycerol.

Cysteine mutants of Sso1pHT were spin-labeled while the proteins were bound to the beads. About a 20-fold excess of (1-oxyl-2,2,5,5-tetramethyl-pyrrolinyl-3-methyl)-methanethiosulfonate spin label (MTSSL) was added to the column. The reaction mixture was left overnight at 4 °C. Free MTSSL was removed by washing with excess PBS buffer containing 0.2% (v/v) Triton X-100. The protein was cleaved by thrombin with 0.2% (v/v) Triton X-100 or 0.8% (w/v) *n*-octylglucoside.

Labeling of the Sso1pHT and Snc2p cysteine mutants with fluorescent probes was carried out after thrombin cleavage. Sso1pHT E185C and Sso1pHT R290C proteins were labeled with Cy3 maleimide; Snc2p P13C and Snc2p S115C were labeled with Cy5 maleimide (Amersham). Free dyes were removed from the proteins by using PD-10 desalting columns (Amersham).

The $His_6$-tagged protein Sec9c was expressed in *E. coli* Rosetta (DE3) pLysS. For purification, the frozen cell pellet was resuspended in lysis buffer (PBS with 20 mM imidazole, 0.2% (v/v) Triton X-100, 2 mM AEBSF, pH 8.0). After sonication, the supernatant was mixed with nickel–nitrilotriacetic acid–agarose beads (Qiagen) in the lysis buffer. The mixture was nutated for binding at 4 °C for 120 min. After binding, the beads were washed with PBS plus 50 mM imidazole, pH 8.0. Then the protein was eluted with PBS plus 250 mM imidazole, pH 8.0. The proteins were stored at −80 °C with 10% (v/v) glycerol. All purified proteins were examined with 15% SDS-PAGE.

## Membrane reconstitution

Large unilamellar vesicles (~100 nm in diameter) of POPC containing 15 or 35 molar percent DOPS were prepared in a detergent-free HEPES buffer (25 mM HEPES, 100 mM KCl, pH 7.4) using an extruder. The total lipid concentration was 100 mM. To study the stoichiometry of the Sso1pHT TMD oligomer, the proteins were reconstituted into the vesicles by the Bio-Beads method48. The proteins were mixed with the vesicles at a series of lipid:protein molar ratios (400:1, 200:1, 100:1, 50:1). The detergent was removed by treating the sample with Bio-Beads SM2 (Bio-Rad), which were added directly to the sample to 200 mg $ml^{-1}$. After 45 min of nutation, the Bio-Beads were removed from the sample by centrifugation at 10,000*g* for 1 min. The Bio-Beads treatment was repeated three times. The reconstitution efficiency was estimated by determining the protein concentration using EPR before and after reconstitution. The reconstitution efficiency was nearly quantitative.

### Electron paramagnetic resonance data collection

The EPR spectra were collected using the Bruker ESP 300 spectrometer equipped with a loop-gap resonator. The modulation amplitude was set at no greater than one-fourth of the line width. Spectra were collected at room temperature. The data in Figure 1c were fitted with an equation representing equilibrium (Equation 1):

$$\ln C = \frac{\ln K + \ln n + n\ln(1-f) - \ln f}{1-n} \quad (2)$$

### Lipid mixing assay

Sso1pHT was reconstituted into vesicles containing POPC and DOPS (molar ratio 65:35) at a lipid:protein ratio of 200:1. Snc2p was reconstituted into vesicles containing POPC, DOPS, NBD-PS (1,2-dioleoyl-*sn*-glycero-3-phosphoserine-*N*-(7-nitro-2-1,3-benzoxadiazol-4-yl)), and rhodamine-PE (1,2-dioleoyl-*sn*-glycero-3-phosphoethanolamine-*N*-(lissamine rhodamine B sulfonyl)) in a molar ratio of 62:35:1.5:1.5. To measure lipid mixing, the v-SNARE (Snc2p) vesicles were mixed with the t-SNARE (Sso1pHT) vesicles and Sec9c at a ratio of 1:1:1. The final lipid concentration was 1 mM. The fluorescence intensity was monitored with excitation and emission wavelengths of 465 and 530 nm, respectively. The fluorescence signal was recorded by a Varian Cary Eclipse fluorescence spectrophotometer using a 100-μl quartz cell with a 2-mm path length. After 3,600 s, 0.1% (v/v) reduced Triton X-100 was added to obtain the maximum fluorescence intensity. The lipid mixing assay was carried out at 35 °C. The inner leaflet mixing assay was modified from a previously published method41. The details of the method have been described elsewhere29. After collecting the time traces of total lipid mixing ($P_T$) and inner leaflet mixing ($P_I$) separately, the time trace for outer leaflet mixing was calculated as $2P_T - P_I$, where $P_T$ is the percentage of maximum for total lipid mixing and $P_I$ is the percentage of maximum for inner leaflet mixing.

### Fluorescence assay for SNARE assembly and self-quenching

Preparation for the fusion reaction was nearly identical to that described above for the lipid mixing assay, except that the vesicles did not contain lipid dyes. The lipid: protein ratio was 200:1 and the final lipid concentration was 1 mM. The fluorescence intensity was monitored in two channels with an excitation wavelength of 555 nm and emission wavelengths of 570 and 668 nm, respectively. To measure self-quenching, fluorescence intensity was monitored with excitation and emission wavelengths of 555 and 570 nm for the Cy3-labeled proteins and with excitation and emission wavelengths of 625 and 668 nm for the Cy5 labeled proteins. The data were fitted to the equation for second-order kinetics:

$$F(t) = \frac{C_0^2 k_2 t}{1 + C_0 k_2 t} \quad (3)$$

where $F$ is the fluorescence change, $C_0$ is the initial concentration in the vesicle and $k_2$ is the second-order rate constant.

## Supplementary Material

Refer to Web version on PubMed Central for supplementary material.

## Acknowledgments

Support for this work was provided by the US National Institutes of Health.

## References

1. Ungar D, Hughson FM. SNARE protein structure and function. Annu Rev Cell Dev Biol. 2003; 19:493–517. [PubMed: 14570579]
2. Brunger AT. Structural insights into the molecular mechanism of calcium-dependent vesicle–membrane fusion. Curr Opin Struct Biol. 2001; 11:163–173. [PubMed: 11297924]
3. Jahn R, Lang T, Sudhof TC. Membrane fusion. Cell. 2003; 112:519–533. [PubMed: 12600315]
4. Rothman JE. Mechanisms of intracellular protein transport. Nature. 1994; 372:55–63. [PubMed: 7969419]
5. Poirier MA, et al. The synaptic SNARE complex is a parallel four-stranded helical bundle. Nat Struct Biol. 1998; 5:765–769. [PubMed: 9731768]
6. Sutton RB, Fasshauer D, Jahn R, Brunger AT. Crystal structure of a SNARE complex involved in synaptic exocytosis at 2.4 Å resolution. Nature. 1998; 395:347–353. [PubMed: 9759724]
7. Hanson PI, Roth R, Morisaki H, Jahn R, Heuser JE. Structure and conformational changes in NSF and its membrane receptor complexes visualized by quick-freeze/deep-etch electron microscopy. Cell. 1997; 90:523–535. [PubMed: 9267032]
8. Lin RC, Scheller RH. Structural organization of the synaptic exocytosis core complex. Neuron. 1997; 19:1087–1094. [PubMed: 9390521]
9. Katz L, Hanson PI, Heuser JE, Brennwald P. Genetic and morphological analyses reveal a critical interaction between the C-termini of two SNARE proteins and a parallel four helical arrangement for the exocytic SNARE complex. EMBO J. 1998; 17:6200–6209. [PubMed: 9799229]
10. Antonin W, Fasshauer D, Becker S, Jahn R, Schneider TR. Crystal structure of the endosomal SNARE complex reveals common structural principles of all SNAREs. Nat Struct Biol. 2002; 9:107–111. [PubMed: 11786915]
11. Strop P, Kaiser SE, Vrljic M, Brunger AT. The structure of the yeast plasma membrane SNARE complex reveals destabilizing water filled cavities. J Biol Chem. 2008; 283:1113–1119. [PubMed: 17956869]
12. Hua Y, Scheller RH. Three SNARE complexes cooperate to mediate membrane fusion. Proc Natl Acad Sci USA. 2001; 98:8065–8070. [PubMed: 11427709]
13. Otto H, Hanson PI, Jahn R. Assembly and disassembly of a ternary complex of synaptobrevin, syntaxin, and SNAP-25 in the membrane of synaptic vesicles. Proc Natl Acad Sci USA. 1997; 94:6197–6201. [PubMed: 9177194]
14. Rickman C, Hu K, Carroll J, Davletov B. Self-assembly of SNARE fusion proteins into star-shaped oligomers. Biochem J. 2005; 388:75–79. [PubMed: 15877547]
15. Hayashi T, et al. Synaptic vesicle membrane fusion complex: action of clostridial neurotoxins on assembly. EMBO J. 1994; 13:5051–5061. [PubMed: 7957071]
16. Chen YA, Scales SJ, Patel SM, Doung YC, Scheller RH. SNARE complex formation is triggered by $Ca^{2+}$ and drives membrane fusion. Cell. 1999; 97:165–174. [PubMed: 10219238]
17. Chernomordik LV, Kozlov MM. Protein-lipid interplay in fusion and fission of biological membranes. Annu Rev Biochem. 2003; 72:175–207. [PubMed: 14527322]
18. Langosch D, Hofmann M, Ungermann C. The role of transmembrane domains in membrane fusion. Cell Mol Life Sci. 2007; 64:850–864. [PubMed: 17429580]
19. Bowen ME, Engelman DM, Brunger AT. Mutational analysis of synaptobrevin transmembrane domain oligomerization. Biochemistry. 2002; 41:15861–15866. [PubMed: 12501216]

20. Laage R, Rohde J, Brosig B, Langosch D. A conserved membrane-spanning amino acid motif drives homomeric and supports heteromeric assembly of presynaptic SNARE proteins. J Biol Chem. 2000; 275:17481–17487. [PubMed: 10764817]
21. Han X, Wang CT, Bai J, Chapman ER, Jackson MB. Transmembrane segments of syntaxin line the fusion pore of $Ca^{2+}$-triggered exocytosis. Science. 2004; 304:289–292. [PubMed: 15016962]
22. Margittai M, Otto H, Jahn R. A stable interaction between syntaxin 1a and synaptobrevin 2 mediated by their transmembrane domains. FEBS Lett. 1999; 446:40–44. [PubMed: 10100611]
23. Chow RH, von Ruden L, Neher E. Delay in vesicle fusion revealed by electrochemical monitoring of single secretory events in adrenal chromaffin cells. Nature. 1992; 356:60–63. [PubMed: 1538782]
24. Wang P, Wang CT, Bai J, Jackson MB, Chapman ER. Mutations in the effector binding loops in the C2A and C2B domains of synaptotagmin I disrupt exocytosis in a nonadditive manner. J Biol Chem. 2003; 278:47030–47037. [PubMed: 12963743]
25. Yoon TY, Okumus B, Zhang F, Shin YK, Ha T. Multiple intermediates in SNARE-induced membrane fusion. Proc Natl Acad Sci USA. 2006; 103:19731–19736. [PubMed: 17167056]
26. Abdulreda MH, Bhalla A, Chapman ER, Moy VT. Atomic force microscope spectroscopy reveals a hemifusion intermediate during soluble *N*-ethylmaleimide-sensitive factor-attachment protein receptors-mediated membrane fusion. Biophys J. 2008; 94:648–655. [PubMed: 17872963]
27. Liu T, Wang T, Chapman E, Weisshaar J. Productive hemifusion intermediates in fast vesicle fusion driven by neuronal SNAREs. Biophys J. 2008; 94:1303–1314. [PubMed: 17951297]
28. Xu Y, Zhang F, Su Z, McNew JA, Shin YK. Hemifusion in SNARE-mediated membrane fusion. Nat Struct Mol Biol. 2005; 12:417–422. [PubMed: 15821745]
29. Lu X, Zhang F, McNew JA, Shin YK. Membrane fusion induced by neuronal SNAREs transits through hemifusion. J Biol Chem. 2005; 280:30538–30541. [PubMed: 15980065]
30. Reese C, Heise F, Mayer A. Trans-SNARE pairing can precede a hemifusion intermediate in intracellular membrane fusion. Nature. 2005; 436:410–414. [PubMed: 15924133]
31. Wong JL, Koppel DE, Cowan AE, Wessel GM. Membrane hemifusion is a stable intermediate of exocytosis. Dev Cell. 2007; 12:653–659. [PubMed: 17420001]
32. Hofmann MW, et al. Self-interaction of a SNARE transmembrane domain promotes the hemifusion-to-fusion transition. J Mol Biol. 2006; 364:1048–1060. [PubMed: 17054985]
33. Giraudo CG, et al. SNAREs can promote complete fusion and hemifusion as alternative outcomes. J Cell Biol. 2005; 170:249–260. [PubMed: 16027221]
34. Zampighi GA, et al. Conical electron tomography of a chemical synapse: vesicles docked to the active zone are hemi-fused. Biophys J. 2006; 91:2910–2918. [PubMed: 16877508]
35. Monck JR, Fernandez JM. The exocytotic fusion pore and neurotransmitter release. Neuron. 1994; 12:707–716. [PubMed: 7909233]
36. Mayer A. What drives membrane fusion in eukaryotes? Trends Biochem Sci. 2001; 26:717–723. [PubMed: 11738595]
37. Jackson MB, Chapman ER. Fusion pores and fusion machines in $Ca^{2+}$-triggered exocytosis. Annu Rev Biophys Biomol Struct. 2006; 35:135–160. [PubMed: 16689631]
38. Lindau M, Almers W. Structure and function of fusion pores in exocytosis and ectoplasmic membrane fusion. Curr Opin Cell Biol. 1995; 7:509–517. [PubMed: 7495570]
39. Jackson MB. In search of the fusion pore of exocytosis. Biophys Chem. 2007; 126:201–208. [PubMed: 16797829]
40. Zhang Y, Shin YK. Transmembrane organization of yeast syntaxin-analogue Sso1p. Biochemistry. 2006; 45:4173–4181. [PubMed: 16566591]
41. Meers P, Ali S, Erukulla R, Janoff AS. Novel inner monolayer fusion assays reveal differential monolayer mixing associated with cation-dependent membrane fusion. Biochim Biophys Acta. 2000; 1467:227–243. [PubMed: 10930525]
42. Li F, et al. Energetics and dynamics of SNAREpin folding across lipid bilayers. Nat Struct Mol Biol. 2007; 14:890–896. [PubMed: 17906638]
43. Tokumaru H, et al. SNARE complex oligomerization by synaphin/complexin is essential for synaptic vesicle exocytosis. Cell. 2001; 104:421–432. [PubMed: 11239399]

44. Yersin A, et al. Interactions between synaptic vesicle fusion proteins explored by atomic force microscopy. Proc Natl Acad Sci USA. 2003; 100:8736–8741. [PubMed: 12853568]
45. Nazarov PV, Koehorst RB, Vos WL, Apanasovich VV, Hemminga MA. FRET study of membrane proteins: determination of the tilt and orientation of the N-terminal domain of M13 major coat protein. Biophys J. 2007; 92:1296–1305. [PubMed: 17114224]
46. Zhuang X, et al. Fluorescence quenching: a tool for single-molecule protein-folding study. Proc Natl Acad Sci USA. 2000; 97:14241–14244. [PubMed: 11121030]
47. Ha T, Xu J. Photodestruction intermediates probed by an adjacent reporter molecule. Phys Rev Lett. 2003; 90:223002. [PubMed: 12857312]
48. Chen Y, Xu Y, Zhang F, Shin YK. Constitutive versus regulated SNARE assembly: a structural basis. EMBO J. 2004; 23:681–689. [PubMed: 14765122]

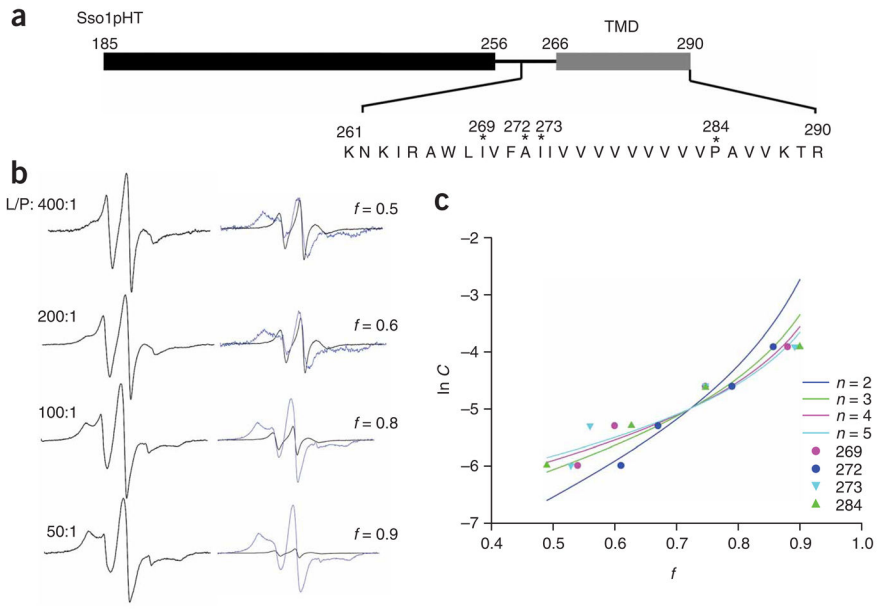


**Figure 1.**

Determination of stoichiometry of the Sso1pHT TMD oligomer using EPR. (**a**) The primary structure of Sso1pHT. Sso1pHT contains amino acids 185–290 of Sso1p and includes both the SNARE motif and the transmembrane domain (black and gray, respectively). The amino acid sequence of part of the linker region and the transmembrane domain is shown. Asterisks, positions selected for EPR analysis. (**b**) EPR spectra of I273C collected at several lipid:protein (L/P) ratios. Each spectrum is decomposed into a sharp (black trace) and a broad EPR component (blue trace). *f*, fraction of oligomeric Sso1pHT. (**c**) Natural log of the protein:lipid ratios (ln *C*) plotted versus *f* for each spin-labeled mutant. The data were fitted with equation 2. The best-fitting values of *n* and ln *K* were 4 and 18.4, respectively (black trace). For comparison, the curves representing $n = 2$ through $n = 5$ are shown.

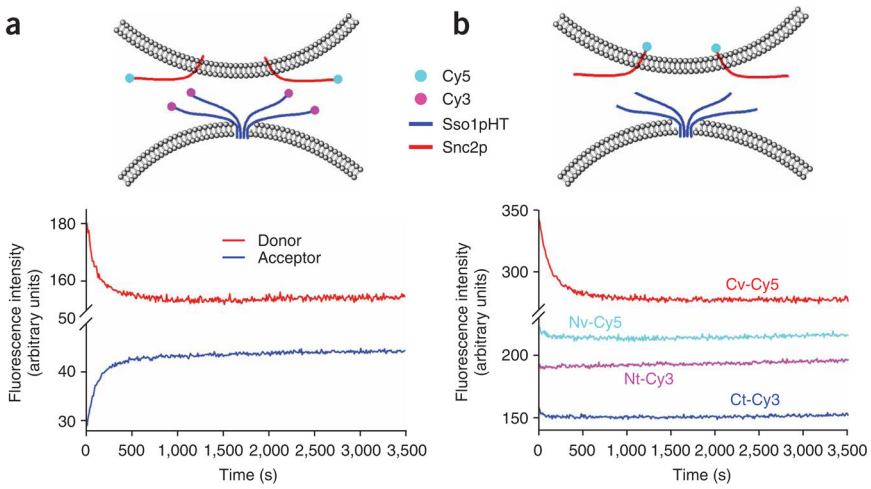


**Figure 2.**

Fluorescence detection of SNARE assembly at different locations. (**a**) SNARE complex formation monitored at the N termini. The fusion reaction was initiated by adding Sec9c to the mixture of the t-SNARE vesicles containing Nt-Cy3 and the v-SNARE vesicles carrying Nv-Cy5 (top panel). Bottom, fluorescence changes for the acceptor channel (blue trace) and for the donor channel (red trace). (**b**) Self-quenching occurs for C-terminally labeled Snc2p owing to clustering of the v-SNARE TMDs in the membrane. Self-quenching was detected by the fluorescence changes when vesicles reconstituted with Cv-Cy5 were mixed with vesicles carrying unlabeled Sso1pHT and Sec9c (red trace). In contrast, we did not observe fluorescence changes in the same assay for the other three labeled proteins: Nt-Cy3 (pink), Ct-Cy3 (blue) and Nv-Cy5 (cyan).

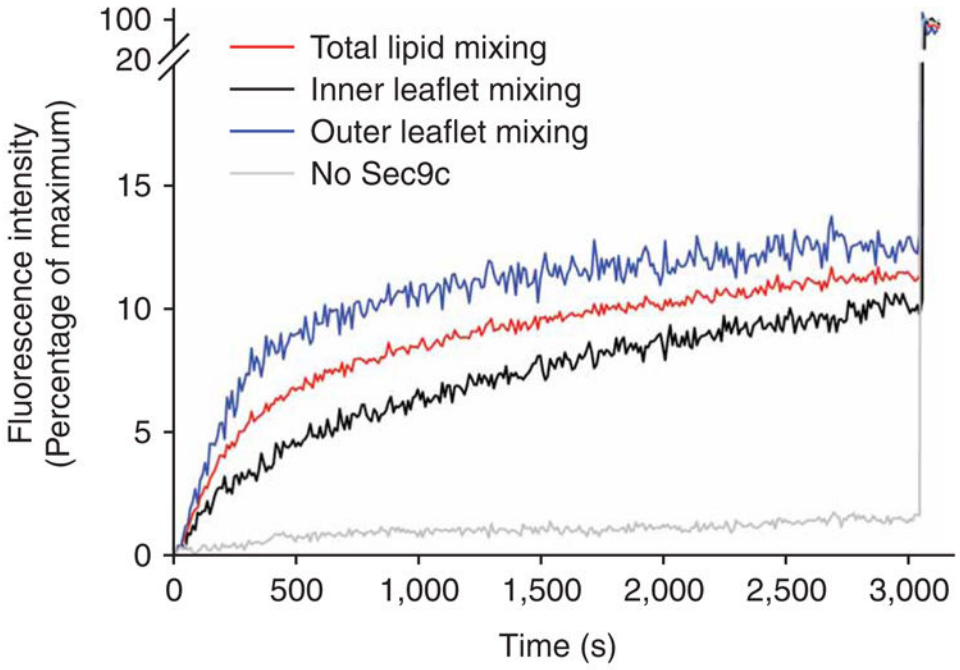


**Figure 3.**

Fluorescence lipid-mixing assay. Fluorescence changes for total lipid mixing (red), inner leaflet mixing (black) and outer leaflet mixing (blue), normalized with respect to the maximum fluorescence intensity (MFI), are shown for the lipid:protein ratio of 200:1. Outer leaflet mixing was calculated from the other two values by subtraction29. Gray trace, control run with the t-SNARE vesicles and the v-SNARE vesicles without Sec9c.

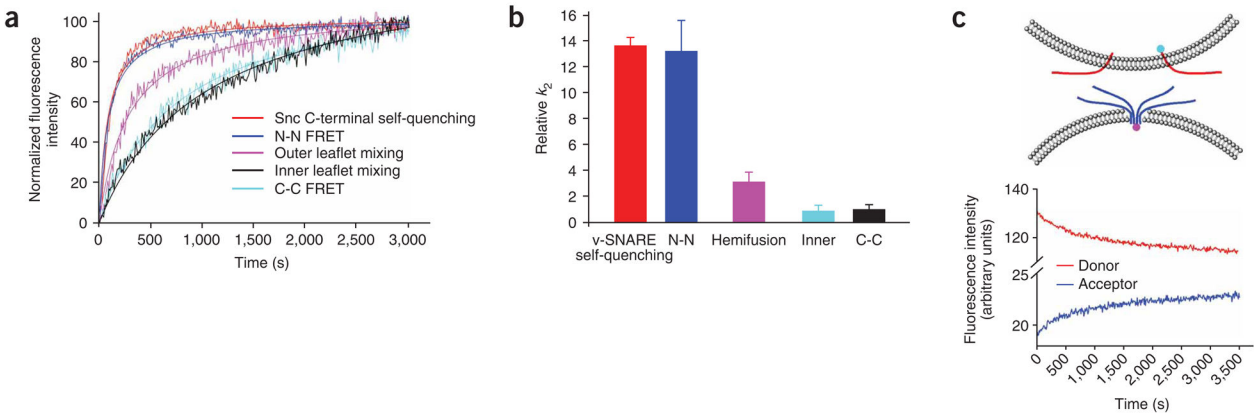


**Figure 4.**

Kinetic comparison of various fluorescence assays. (**a**) Analysis of various fluorescence assays based on second-order kinetics. Red trace, Cv-Cy5 self-quenching kinetics; blue trace, assembly kinetics of the Nt-Cy3–Nv-Cy5 complex (N-N); pink trace, outer leaflet mixing; black trace, inner leaflet mixing; cyan trace, kinetics of *cis*-SNARE complex (C-C) formation. The solid line in each trace is the best fit to equation 3. For the individual time traces, the fluorescence intensities at 3,000 s were normalized to 100 in arbitrary units. Colors are the same as in Figure 2. (**b**) Graph of the relative $k_2$ values for different kinetic traces. Error bars, s.d. of three independent measurements. The $k_2$ value for inner leaflet mixing was set at 1 and those for the other kinetics were scaled accordingly. (**c**) Measurement of *cis*-SNARE complex formation using fluorescence. Vesicles reconstituted with the mixture of Cv-Cy5 and unlabeled Snc2p in a 1:3 ratio were reacted with vesicles containing Ct-Cy3 and unlabeled Sso1pHT in a 1:3 ratio by adding Sec9c (top panel). Bottom, fluorescence changes were observed for acceptor channel (blue) and donor channel (red).

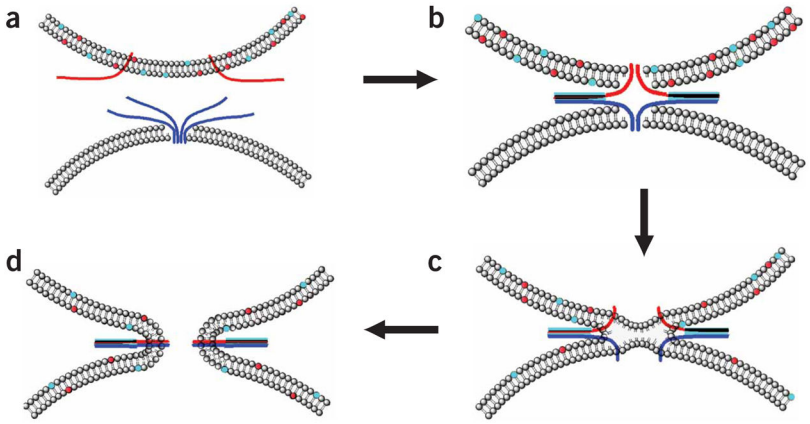


**Figure 5.**

A mechanistic model for SNARE assembly and membrane fusion. (**a**) v-SNARE on the vesicle (red) and t-SNARE on target membrane (blue) interact to facilitate the apposition of two membranes. The t-SNARE TMDs form an oligomeric structure in the membrane. (**b**) The Sso1pHT homo-oligomer provides scaffolding for formation of the supramolecular SNARE complex at the fusion site. (**c**) Hemifusion. (**d**) Fusion pore opening coincides with *cis*-SNARE complex formation. Cyan dots and red dots, NBD- and rhodamine-labeled groups, respectively.